Supporting Information for Fast Burst-Sparsity Learning Based Baseline Correction (FBSL-BC) Algorithm for Signals of Analytical Instruments

Haoran Li,† Suyi Chen,† Jisheng Dai,*,† Xiaobo Zou,*,‡ Tao Chen,¶ Tianhong Pan,§ and Melvin Holmes‖

†*School of Electrical and Information Engineering, Jiangsu University, Zhenjiang 212013, China*

‡*School of Food and Biological Engineering, Jiangsu University, Zhenjiang 212013, China*

¶*Department of Chemical and Process Engineering, University of Surrey, Guildford GU2 7XH, United Kingdom*

§*School of Electrical Engineering and Automation, Anhui University, Hefei, 230061, China*

‖*School of Food Science and Nutrition, University of Leeds, Leeds LS2 9JT, United Kingdom*

E-mail: jsdai@ujs.edu.cn; xiaobo@ujs.edu.cn

Supporting Information Contents

Figures

Tables

Table S-1: Comparison of averaged RMSECV among airPLS ($\lambda^{\mathrm{air}} = 10^8$), arPLS ($\lambda^{\mathrm{ar}} = 10^5$), SSFBCSP ($\lambda_1 = 10^4$ and $\lambda_2 = 10^{-2}$), SBL-BC ($\rho = 10^5$) and FBSL-BC.

Table S-2:Comparison of averaged RMSEP results among airPLS ($\lambda^{\mathrm{air}} = 10^8$), arPLS ($\lambda^{\mathrm{ar}} = 10^5$), SSFBCSP ($\lambda_1 = 2 \times 10^5$ and $\lambda_2 = 10^{-2}$), SBL-BC ($\rho = 10^5$) and FBSL-BC.

The proof of Lemma 1

Lemma. 1: The optimal solutions to (20)–(25) are given as follows:

$$q^{(r+1)}(\mathbf{W}) = \prod_{g=1}^{G} \mathcal{N}(\mathbf{w}_g|\hat{\mathbf{w}}_g^{(r+1)}, \boldsymbol{\Sigma}^{(r+1)}), \tag{1}$$

$$q^{(r+1)}(\alpha) = \Gamma\Big(\alpha\Big|e + \frac{1}{2}LG, f_\alpha^{(r+1)}\Big), \tag{2}$$

$$q^{(r+1)}(\boldsymbol{\gamma}) = \prod_{l=1}^{L} \Gamma\Big(\gamma_l\Big|e_l^{(r+1)}, f_l^{(r+1)}\Big), \tag{3}$$

$$q^{(r+1)}(\mathbf{h}) = \prod_{l=1}^{L} \prod_{k\in\{-1,0,1\}} \hat{h}_{l,k}^{(r+1)} \delta(h_l - k), \tag{4}$$

$$q^{(r+1)}(\beta) = \Gamma\left(\beta\Big|e + \frac{1}{2}LG, f_\beta^{(r+1)}\right), \tag{5}$$

$$q^{(r+1)}(\mathbf{B}) = \prod_{g=1}^{G} \mathcal{N}\left(\mathbf{b}_g\Big|\hat{\mathbf{b}}_g^{(r+1)}, \boldsymbol{\Sigma}_b^{(r+1)}\right), \tag{6}$$

where

$$\boldsymbol{\Sigma}^{(r+1)} =\Big(\hat{\alpha}^{(r)}\mathbf{A}_L^{\mathrm{T}}\mathbf{A}_L + \sum_{k\in\{-1,0,1\}} \boldsymbol{\Psi}_k^{(r)}\boldsymbol{\Lambda}_k^{(r)}\Big)^{-1}, \tag{7}$$

$$\hat{\mathbf{w}}_g^{(r+1)} =\hat{\alpha}^{(r)}\boldsymbol{\Sigma}^{(r+1)}\mathbf{A}_L^{\mathrm{T}}(\mathbf{x}_g - \hat{\mathbf{b}}_g^{(r)}), \tag{8}$$

$$f_\alpha^{(r+1)} =f + \frac{1}{2}\sum_{g=1}^{G}\Big(\|\mathbf{x}_g - \mathbf{A}_L\hat{\mathbf{w}}_g^{(r+1)} - \hat{\mathbf{b}}_g^{(r)}\|_2^2 + \mathrm{tr}\{\mathbf{A}_L\boldsymbol{\Sigma}^{(r+1)}\mathbf{A}_L^{\mathrm{T}} + \boldsymbol{\Sigma}_b^{(r)}\}\Big), \tag{9}$$

$$\hat{\alpha}^{(r+1)} = \langle\alpha\rangle_{q^{(r+1)}(\alpha)} = (e + \frac{1}{2}LG)/f_\alpha^{(r+1)}, \tag{10}$$

$$e_l^{(r+1)} =e + \frac{G}{2}\big(\hat{h}_{l+1,-1}^{(r)} + \hat{h}_{l,0}^{(r)} + \hat{h}_{l-1,1}^{(r)}\big), \tag{11}$$

$$f_l^{(r+1)} =f + \frac{1}{2}\sum_{g=1}^{G}\big(\hat{h}_{l+1,-1}^{(r)}\varpi_{l+1,g}^{(r+1)} + \hat{h}_{l,0}^{(r)}\varpi_{l,g}^{(r+1)} + \hat{h}_{l-1,1}^{(r)}\varpi_{l-1,g}^{(r+1)}\big), \tag{12}$$

$$\hat{\gamma}_l^{(r+1)} = \langle\gamma_l\rangle_{q^{(r+1)}(\gamma_l)} = e_l^{(r+1)}/f_l^{(r+1)}, \tag{13}$$

$$\hat{h}_{l,k}^{(r+1)} = \frac{\exp(\nu_{l,k}^{(r+1)})}{\sum_{k\in\{-1,0,1\}}\exp(\nu_{l,k}^{(r+1)})}, \tag{14}$$

$$f_\beta^{(r+1)} = f + \frac{1}{2}\sum_{g=1}^{G}\Big(\|\mathbf{D}_L\hat{\mathbf{b}}_g^{(r)}\|^2 + \mathrm{tr}\{\mathbf{D}_L\boldsymbol{\Sigma}_b^{(r)}\mathbf{D}_L^{\mathrm{T}}\}\Big), \tag{15}$$

$$\hat{\beta}^{(r+1)} = \langle\beta\rangle_{q^{(r+1)}(\beta)} = (e + \frac{1}{2}LG)/(f_\beta^{(r+1)}), \tag{16}$$

$$\boldsymbol{\Sigma}_b^{(r+1)} = \Big(\hat{\alpha}^{(r+1)}\mathbf{I} + \hat{\beta}^{(r+1)}\mathbf{D}_L^{\mathrm{T}}\mathbf{D}_L\Big)^{-1}, \tag{17}$$

$$\hat{\mathbf{b}}_g^{(r+1)} = \hat{\alpha}^{(r+1)}\boldsymbol{\Sigma}_b^{(r+1)}\Big(\mathbf{x}_g - \mathbf{A}_L\hat{\mathbf{w}}_g^{(r+1)}\Big). \tag{18}$$

with $\boldsymbol{\Psi}_k^{(r)} = \mathrm{diag}\{\hat{h}_{1,k}^{(r)}, \hat{h}_{2,k}^{(r)}, \ldots, \hat{h}_{L,k}^{(r)}\}$, $\boldsymbol{\Lambda}_k^{(r)} = \mathrm{diag}\{\hat{\gamma}_{1+k}^{(r)}, \hat{\gamma}_{2+k}^{(r)}, \ldots, \hat{\gamma}_{L+k}^{(r)}\}$, $\varpi_{l,g}^{(r+1)} = \left\langle w_{l,j}^2\right\rangle_{q^{(r+1)}(w_j)} = [\hat{w}_{l,g}^{(r+1)}]_j^2 + [\boldsymbol{\Sigma}^{(r+1)}]_{l,l}$, $\nu_{l,k}^{(r+1)} = \frac{G}{2}\big(\widehat{\ln\gamma_{l+k}}\big)^{(r+1)} - \frac{1}{2}\sum_{g=1}^{G}\hat{\gamma}_{l+k}^{(r+1)}\varpi_{l,g}^{(r+1)}$, and $\big(\widehat{\ln\gamma_l}\big)^{(r+1)} = \langle\ln\gamma_l\rangle_{q^{(r+1)}(\gamma_l)} = \Psi(e_l^{(r+1)}) - \ln(f_l^{(r+1)})$.

Proof. The joint distribution $p(\mathbf{X}, \mathbf{W}, \mathbf{h}, \boldsymbol{\gamma}, \mathbf{B}, \alpha, \beta)$ can be factorized by

$$p(\mathbf{X}, \mathbf{W}, \mathbf{h}, \boldsymbol{\gamma}, \mathbf{B}, \alpha, \beta) = p\left(\mathbf{X}|\mathbf{W}, \mathbf{B}, \alpha\right)p(\mathbf{W}|\boldsymbol{\gamma}, \mathbf{h})p(\boldsymbol{\gamma})p(\mathbf{h})p(\mathbf{B}|\beta)p(\beta)p(\alpha) \tag{19}$$

The stationary solution can be obtained by following iteratively update strategy:

$$\ln q^{(r+1)}(\Omega_1) \propto \langle\ln p\left(\mathbf{X}, \Omega\right)\rangle_{q^{(r)}(\Omega_2)q^{(r)}(\Omega_3)q^{(r)}(\Omega_4)q^{(r)}(\Omega_5)q^{(r)}(\Omega_6)}, \tag{20}$$

$$\ln q^{(r+1)}(\Omega_2) \propto \langle\ln p\left(\mathbf{X}, \Omega\right)\rangle_{q^{(r+1)}(\Omega_1)q^{(r)}(\Omega_3)q^{(r)}(\Omega_4)q^{(r)}(\Omega_5)q^{(r)}(\Omega_6)}, \tag{21}$$

$$\ln q^{(r+1)}(\Omega_3) \propto \langle\ln p\left(\mathbf{X}, \Omega\right)\rangle_{q^{(r+1)}(\Omega_1)q^{(r+1)}(\Omega_2)q^{(r)}(\Omega_4)q^{(r)}(\Omega_5)q^{(r)}(\Omega_6)}, \tag{22}$$

$$\ln q^{(r+1)}(\Omega_4) \propto \langle\ln p\left(\mathbf{X}, \Omega\right)\rangle_{q^{(r+1)}(\Omega_1)q^{(r+1)}(\Omega_2)q^{(r+1)}(\Omega_3)q^{(r)}(\Omega_5)q^{(r)}(\Omega_6)}, \tag{23}$$

$$\ln q^{(r+1)}(\Omega_5) \propto \langle\ln p\left(\mathbf{X}, \Omega\right)\rangle_{q^{(r+1)}(\Omega_1)q^{(r+1)}(\Omega_2)q^{(r+1)}(\Omega_3)q^{(r+1)}(\Omega_4)q^{(r)}(\Omega_6)}, \tag{24}$$

$$\ln q^{(r+1)}(\Omega_6) \propto \langle\ln p\left(\mathbf{X}, \Omega\right)\rangle_{q^{(r+1)}(\Omega_1)q^{(r+1)}(\Omega_2)q^{(r+1)}(\Omega_3)q^{(r+1)}(\Omega_4)q^{(r+1)}(\Omega_5)}, \tag{25}$$

Substituting (19) into (20), we obtain

$$
\begin{aligned}
&\ln q^{(r+1)}(\mathbf{W}) \\
&\propto \langle \ln p\left(\mathbf{X}|\mathbf{W},\mathbf{B},\alpha\right) p(\mathbf{W}|\boldsymbol{\gamma},\mathbf{h})\rangle_{q^{(r)}(\alpha)q^{(r)}(\boldsymbol{\gamma})q^{(r)}(\mathbf{h})q^{(r)}(\mathbf{B})} && (26)\\
&\propto -\frac{1}{2}\hat{\alpha}^{(r)}\sum_{g=1}^{G}\|\mathbf{x}_g-\mathbf{A}_L\mathbf{w}_g-\hat{\mathbf{b}}_g^{(r)}\|_2^2-\frac{1}{2}\sum_{g=1}^{G}\mathbf{w}_g^{\mathrm{T}}(\boldsymbol{\Psi}_{-1}^{(r)}\boldsymbol{\Lambda}_{-1}^{(r)}+\boldsymbol{\Psi}_{0}^{(r)}\boldsymbol{\Lambda}_{0}^{(r)}+\boldsymbol{\Psi}_{1}^{(r)}\boldsymbol{\Lambda}_{1}^{(r)})\mathbf{w}_g, && (27)
\end{aligned}
$$

where $\boldsymbol{\Psi}_k^{(r)}=\mathrm{diag}\{\hat{h}_{1,k}^{(r)},\hat{h}_{2,k}^{(r)},\ldots,\hat{h}_{L,k}^{(r)}\}$ with $\hat{h}_{l,k}^{(r)}=q^{(r)}(h_l=k)$, $\boldsymbol{\Lambda}_k^{(r)}=\mathrm{diag}\{\hat{\gamma}_{1+k}^{(r)},\hat{\gamma}_{2+k}^{(r)},\ldots,\hat{\gamma}_{L+k}^{(r)}\}$, and $\hat{\mathbf{b}}_g^{(r)}=\langle\mathbf{b}\rangle_{q^{(r)}(\mathbf{b}_g)}$. It shows that $q^{(r+1)}(\mathbf{w}_g)$s are separable and follow Gaussian distributions:

$$
q^{(r+1)}(\mathbf{w}_g)=\mathcal{N}(\mathbf{w}_g|\hat{\mathbf{w}}_g^{(r+1)},\boldsymbol{\Sigma}^{(r+1)}),\quad g=1,2,\cdots,G, \tag{28}
$$

where

$$
\begin{aligned}
\boldsymbol{\Sigma}^{(r+1)} =&\Big(\hat{\alpha}^{(r)}\mathbf{A}_L^{\mathrm{T}}\mathbf{A}_L+\sum_{k\in\{-1,0,1\}}\boldsymbol{\Psi}_k^{(r)}\boldsymbol{\Lambda}_k^{(r)}\Big)^{-1}, && (29)\\
\hat{\mathbf{w}}_g^{(r+1)} =&\hat{\alpha}^{(r)}\boldsymbol{\Sigma}^{(r+1)}\mathbf{A}_L^{\mathrm{T}}(\mathbf{x}_g-\hat{\mathbf{b}}_g^{(r)}). && (30)
\end{aligned}
$$

Substituting (19) into (21), we obtain

$$
\begin{aligned}
&\ln q^{(r+1)}(\alpha) \\
&\propto \langle \ln p\left(\mathbf{X}|\mathbf{W},\mathbf{B},\alpha\right) p(\alpha)\rangle_{q^{(r+1)}(\mathbf{W})q^{(r)}(\mathbf{B})} && (31)\\
&\propto -\frac{1}{2}\alpha\sum_{g=1}^{G}\Big(\|\mathbf{x}_g-\mathbf{A}_L\hat{\mathbf{w}}_g^{(r+1)}-\hat{\mathbf{b}}_g^{(r)}\|_2^2+\mathrm{tr}\{\mathbf{A}_L\boldsymbol{\Sigma}^{(r+1)}\mathbf{A}_L^{\mathrm{T}}+\boldsymbol{\Sigma}_b^{(r)}\}\Big)-\alpha f+(e+LG/2-1)\ln\alpha. && (32)
\end{aligned}
$$

Hence, $q^{(r+1)}(\alpha)$ obeys a Gamma distribution:

$$q^{(r+1)}(\alpha) = \Gamma\Big(\alpha \Big| e + \frac{1}{2}LG, f_\alpha^{(r+1)}\Big), \tag{33}$$

where $f_\alpha^{(r+1)} = f + \frac{1}{2}\sum_{g=1}^{G}\Big(\|\mathbf{x}_g - \mathbf{A}_L\hat{\mathbf{w}}_g^{(r+1)} - \hat{\mathbf{b}}_g^{(r)}\|_2^2 + \mathrm{tr}\{\mathbf{A}_L\boldsymbol{\Sigma}^{(r+1)}\mathbf{A}_L^{\mathrm{T}} + \boldsymbol{\Sigma}_b^{(r)}\}\Big)$.

Substituting (19) into (22), we obtain

$$\begin{aligned}
&\ln q^{(r+1)}(\boldsymbol{\gamma}) \\
\propto& \langle \ln p(\mathbf{W}|\boldsymbol{\gamma}, \mathbf{h}) p(\boldsymbol{\gamma})\rangle_{q^{(r+1)}(\mathbf{W})q^{(r)}(\mathbf{h})} \qquad (34)\\
\propto& \sum_{l=1}^{L} -\gamma_l\Big(f + \frac{1}{2}\sum_{g=1}^{G}\big(\hat{h}_{l+1,-1}^{(r)}\varpi_{l+1,g}^{(r+1)} + \hat{h}_{l,0}^{(r)}\varpi_{l,g}^{(r+1)} + \hat{h}_{l-1,1}^{(r)}\varpi_{l-1,g}^{(r+1)}\big)\Big)\\
&+ \sum_{l=1}^{L}\Big(e + \frac{G}{2}\big(\hat{h}_{l+1,-1}^{(r)} + \hat{h}_{l,0}^{(r)} + \hat{h}_{l-1,1}^{(r)}\big) - 1\Big)\ln\gamma_l. \qquad (35)
\end{aligned}$$

It shows that $q^{(r+1)}(\gamma_l)$s are also separable and follow Gamma distributions:

$$q^{(r+1)}(\gamma_l) = \Gamma\Big(\alpha \Big| e_l^{(r+1)}, f_l^{(r+1)}\Big), \quad l = 1, 2, \cdots, L, \tag{36}$$

where $e_l^{(r+1)} = e + \frac{G}{2}\big(\hat{h}_{l+1,-1}^{(r)} + \hat{h}_{l,0}^{(r)} + \hat{h}_{l-1,1}^{(r)}\big)$ and $f_l^{(r+1)} = f + \frac{1}{2}\sum_{g=1}^{G}\big(\hat{h}_{l+1,-1}^{(r)}\varpi_{l+1,g}^{(r+1)} + \hat{h}_{l,0}^{(r)}\varpi_{l,g}^{(r+1)} + \hat{h}_{l-1,1}^{(r)}\varpi_{l-1,g}^{(r+1)}\big)$.

Substituting (19) into (23), we obtain

$$\ln q^{(r+1)}(\mathbf{h}) \propto \langle \ln p(\mathbf{W}|\boldsymbol{\gamma}, \mathbf{h}) p(\mathbf{h})\rangle_{q^{(r+1)}(\mathbf{W})q^{(r+1)}(\boldsymbol{\gamma})}. \tag{37}$$

Because h_l takes values from $\{-1, 0, 1\}$ only, we can directly calculate $q^{(r+1)}(h_l = k)$, $k \in \{1, 0, 1\}$:

$$\ln q^{(r+1)}(h_l = k) \propto \underbrace{\frac{G}{2}\big(\widehat{\ln\gamma_{l+k}}\big)^{(r+1)} - \frac{1}{2}\sum_{g=1}^{G}\hat{\gamma}_{l+k}^{(r+1)}\varpi_{l,g}^{(r+1)}}_{\triangleq \nu_{l,k}^{(r+1)}}, \tag{38}$$

where $\left(\widehat{\ln \gamma_l}\right)^{(r+1)} = \langle \ln \gamma_l \rangle_{q^{(r+1)}(\gamma_l)} = \Psi(e_l^{(r+1)}) - \ln(f_l^{(r+1)})$. Since $\sum_{k\in\{-1,0,1\}} q^{(r+1)}(h_l = k)$, we have

$$\hat{h}_{l,k}^{(r+1)} = q^{(r+1)}(h_l = k) = \frac{\exp(\nu_{l,k}^{(r+1)})}{\sum_{k\in\{-1,0,1\}} \exp(\nu_{l,k}^{(r+1)})}, \quad k \in \{-1, 0, 1\}. \tag{39}$$

Finally, the update rules for $q^{(r+1)}(\beta)$ and $q^{(r+1)}(\mathbf{B})$ coincide with the ones in , whose proofs are omitted for brevity. □

For the computational efficiency, we can similarly set $\hat{\beta} = \rho\hat{\alpha}^{(r+1)}$ and $\hat{\alpha}^{(r+1)}\mathbf{\Sigma}_b^{(r+1)} = \left(\mathbf{I} + \rho \cdot \mathbf{D}_L^{\mathrm{T}}\mathbf{D}_L\right)^{-1}$, and then (18) can be simplified as:

$$\hat{\mathbf{b}}_g^{(r+1)} = \left(\mathbf{I} + \rho \cdot \mathbf{D}_L^{\mathrm{T}}\mathbf{D}_L\right)^{-1} \left(\mathbf{x}_g - \mathbf{A}_L\hat{\mathbf{w}}_g^{(r+1)}\right), \tag{40}$$

where ρ can be simply choose from $\{10^4, 10^5, 10^7, 10^8\}$

Pseudo Code of FBSL-BC

Algorithm 1 FBSL-BC

1. Input: $\mathbf{x}$ and G.
2. Down-sample $\mathbf{x}$ into $\mathbf{x}_g$s,
3. Initialize $\hat{\alpha}^{(0)}$, $\hat{\boldsymbol{\gamma}}^{(0)}$, $\hat{h}_{l,k}^{(0)}$s, $\boldsymbol{\Sigma}_b^{(0)}$ and $\hat{\mathbf{b}}_g^{(0)}$s, and set $r = 0$, $e = 10^{-10}$ and $f = 10^{-10}$.
4. Repeat the following steps:
   a) Update $\boldsymbol{\Sigma}^{(r+1)}$ and $\hat{\mathbf{w}}_g^{(r+1)}$s using (7) and (8), and then project $\hat{\mathbf{w}}_g^{(r+1)}$s to their non-negative parts.
   b) Update $\hat{\alpha}^{(r+1)}$ using (10) and let $\hat{\alpha}^{(r+1)} = \min\{\hat{\alpha}^{(r+1)}, 10^5\}$.
   c) Update $\hat{\gamma_l}^{(r+1)}$s using (13).
   d) Update $\hat{h}_{l,k}^{(r+1)}$s using (14).
   e) Update $\hat{\mathbf{b}}_g^{(r+1)}$s using (40).
   f) Update σ_l^2s using the variance refinement.
   g) Let $r = r + 1$ and go back to Step-4a until a given threshold is reached.
5. Output: $\hat{\mathbf{w}}_g^{(r)}$s and $\hat{\mathbf{b}}_g^{(r)}$s.

Figures

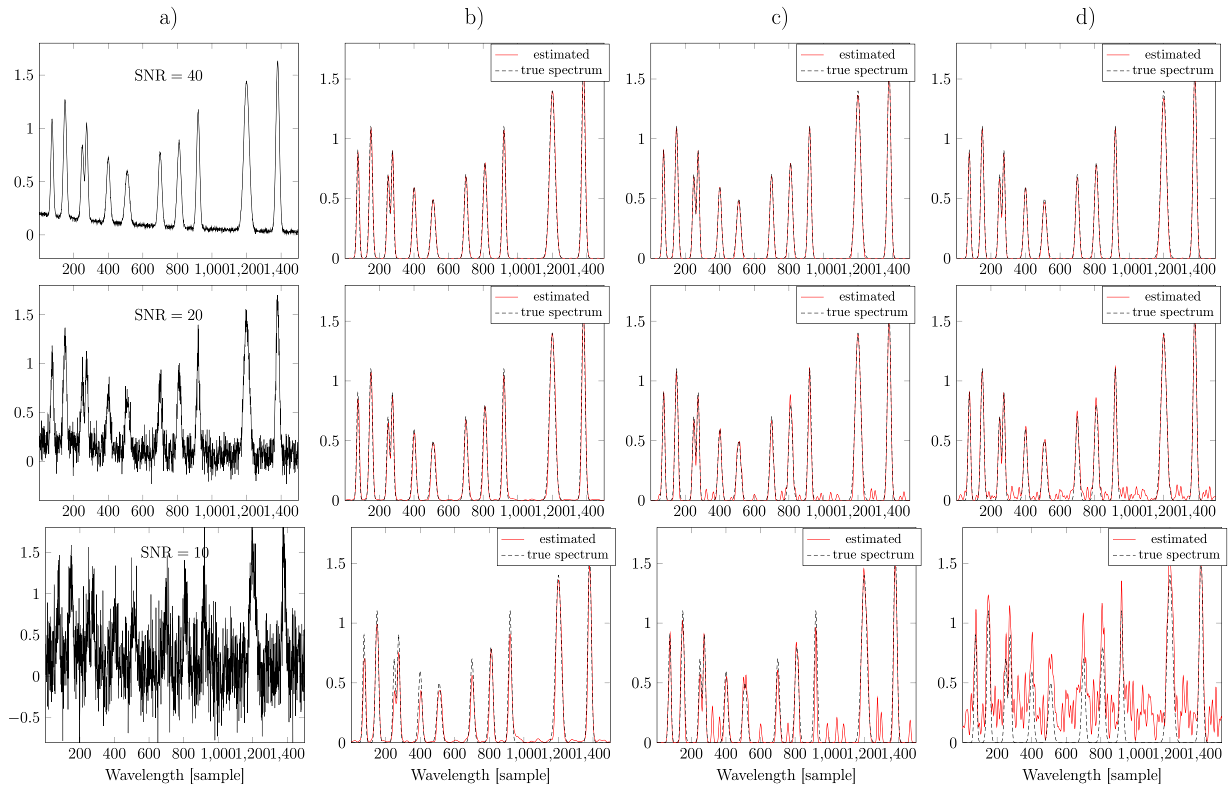

Figure S-1: Comparison among FBSL-BC, SBL-BC and SSFBCSP for simulated spectrum with exponential baseline. a) simulated spectrum, b) FBSL-BC, c) SBL-BC, d) SSFBCSP with $\lambda_1 = \{10^4, 10^6, 10^5\}$ and $\lambda_2 = \{10^{-3}, 10^{-1}, 10^{-1}\}$.

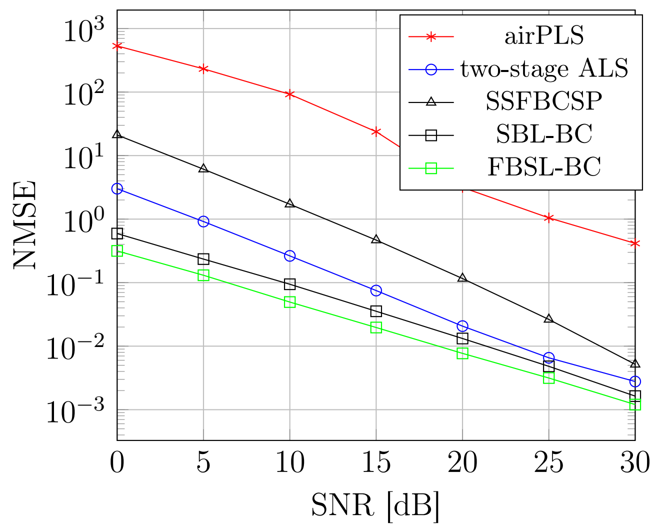

Figure S-2: NMSE results under different SNR for simulated data with exponential baseline, where $\lambda_1 = 10^5$, $\lambda_2 = 10^{-2}$, $\lambda^{\mathrm{ALS}} = 10^5$, $p^{\mathrm{ALS}} = 0.005$ and $\lambda^{\mathrm{air}} = 10^4$.

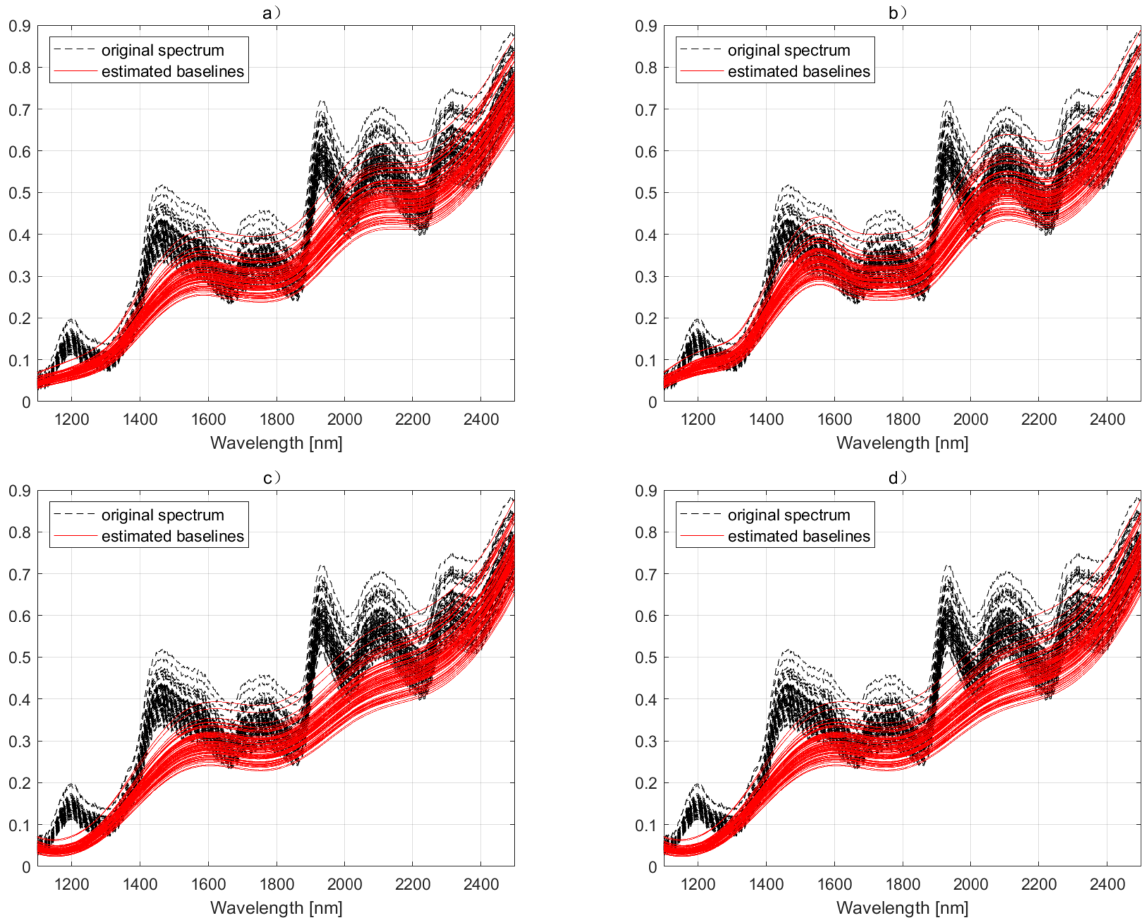

Figure S-3: The corn spectrum (with added noise, SNR = $50dB$) and estimated baseline. a) FBSL-BC, b) SBL-BC, c) SSFBCSP, d) airPLS.

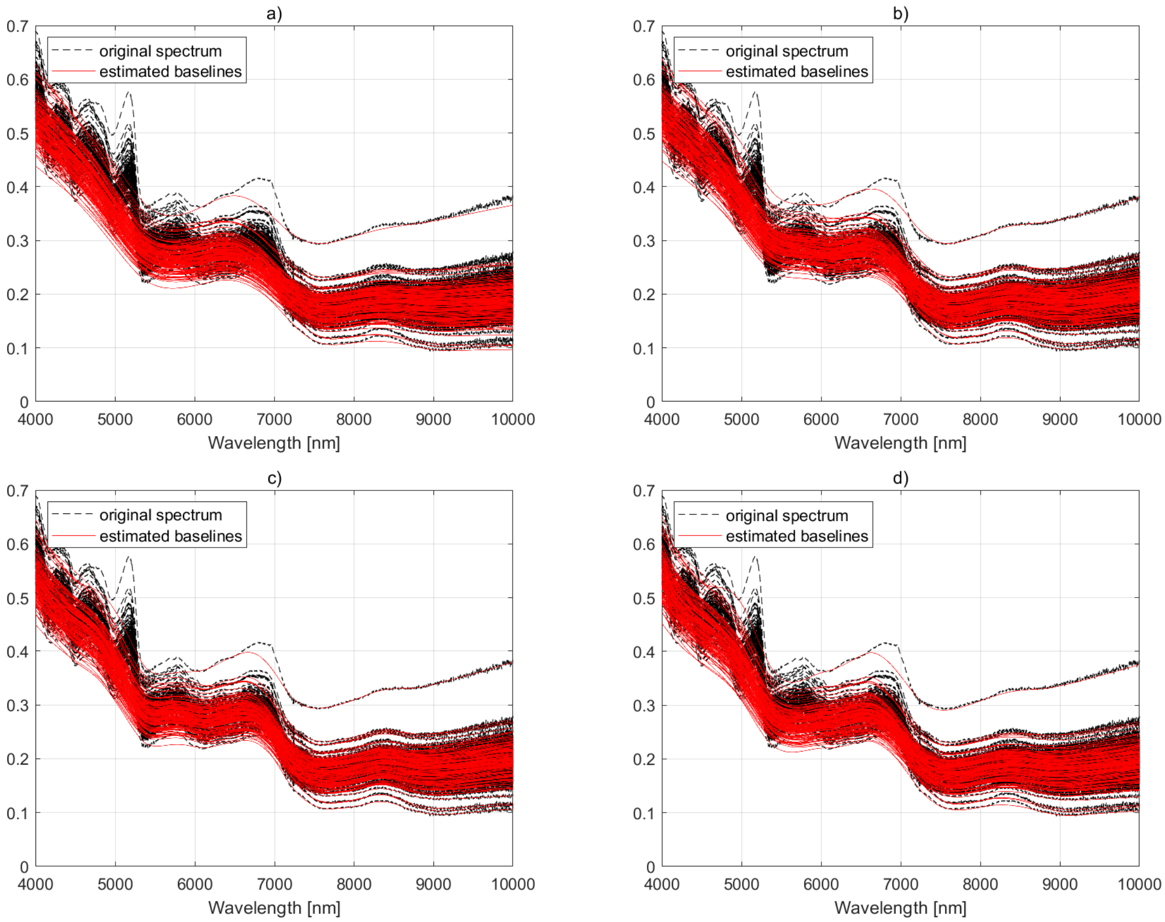

Figure S-4: The original tea spectrum and estimated baseline. a) FBSL-BC, b) SBL-BC, c) SSFBCSP and d) airPLS.

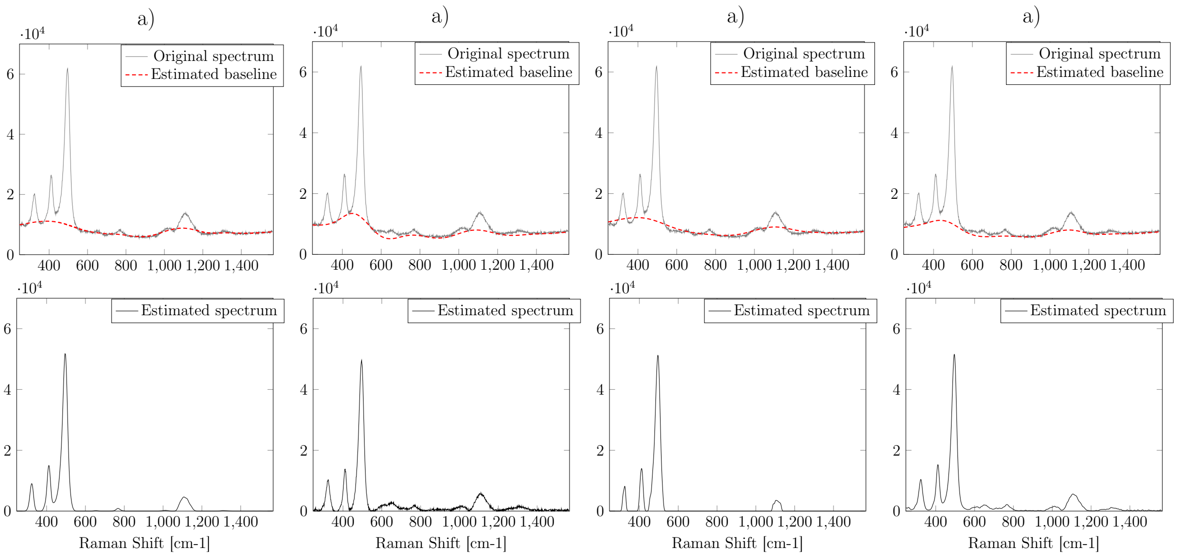

Figure S-5: Comparison of baseline correction results for GmeliniteNa Raman spectral with SNR $= 50dB$. a) FBSL-BC, b) airPLS ($\lambda^{\text{air}} = 10^9$), c) SBL-BC, d) SSFBCSP ($\lambda_1 = 10^6$ and $\lambda_2 = 10^{-2}$).

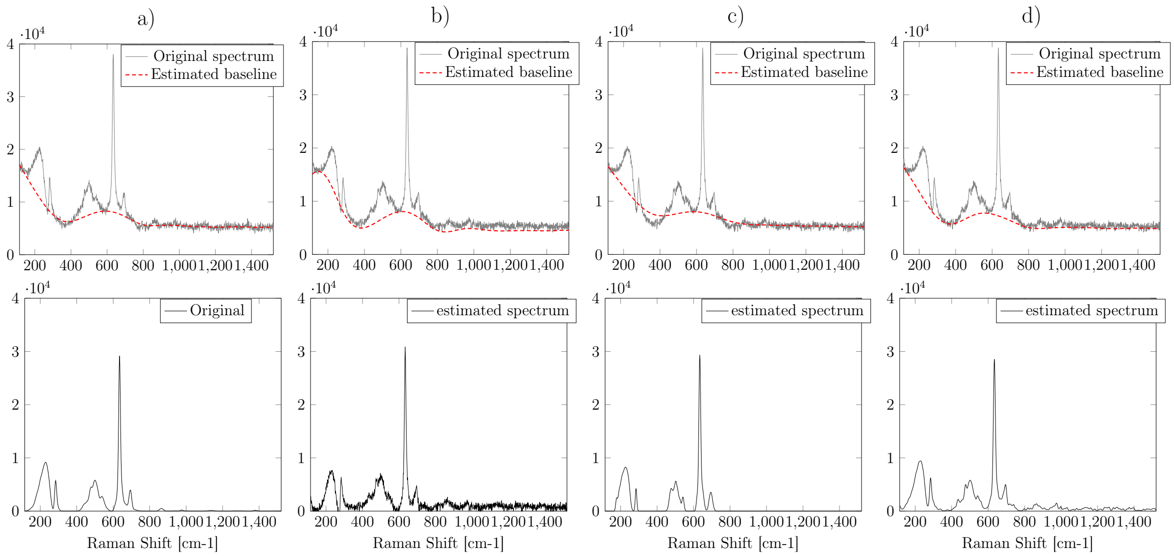

Figure S-6: Comparison of baseline correction results for Cassiterite Raman spectral with SNR $= 40dB$. a) FBSL-BC, b) airPLS ($\lambda^{\text{air}} = 10^9$), c) SBL-BC, d) SSFBCSP ($\lambda_1 = 10^6$ and $\lambda_2 = 10^{-2}$).

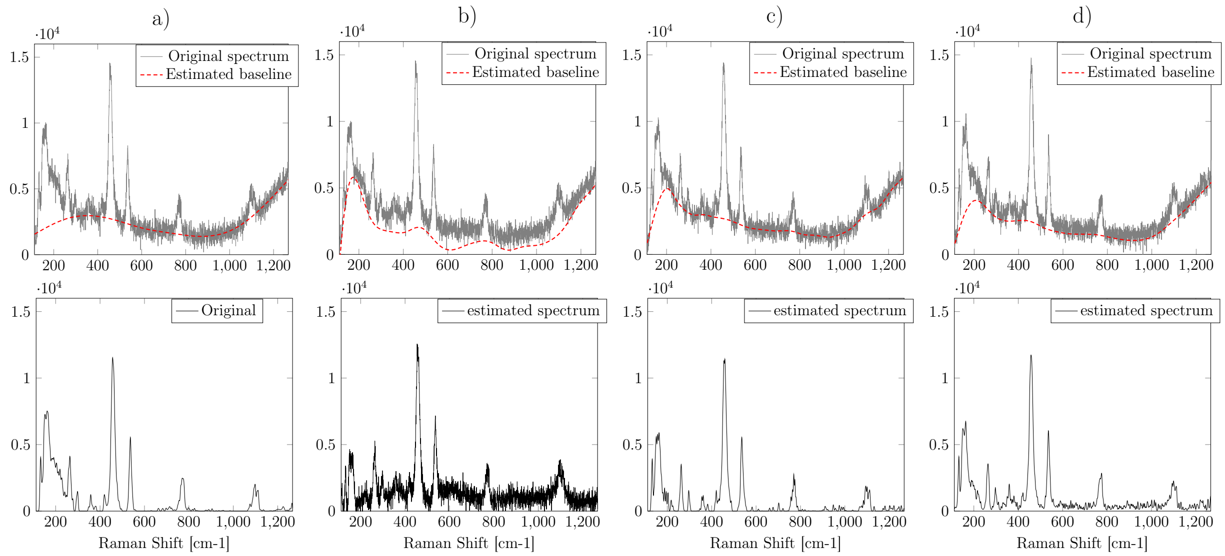

figure S-7: Comparison of baseline correction results for Marialite Raman spectra with SNR $= 30dB$. a) FBSL-BC, b) airPLS ($\lambda^{\mathrm{air}} = 10^9$), c) SBL-BC, d) SSFBCSP ($\lambda_1 = 10^6$ and $\lambda_2 = 10^{-2}$).

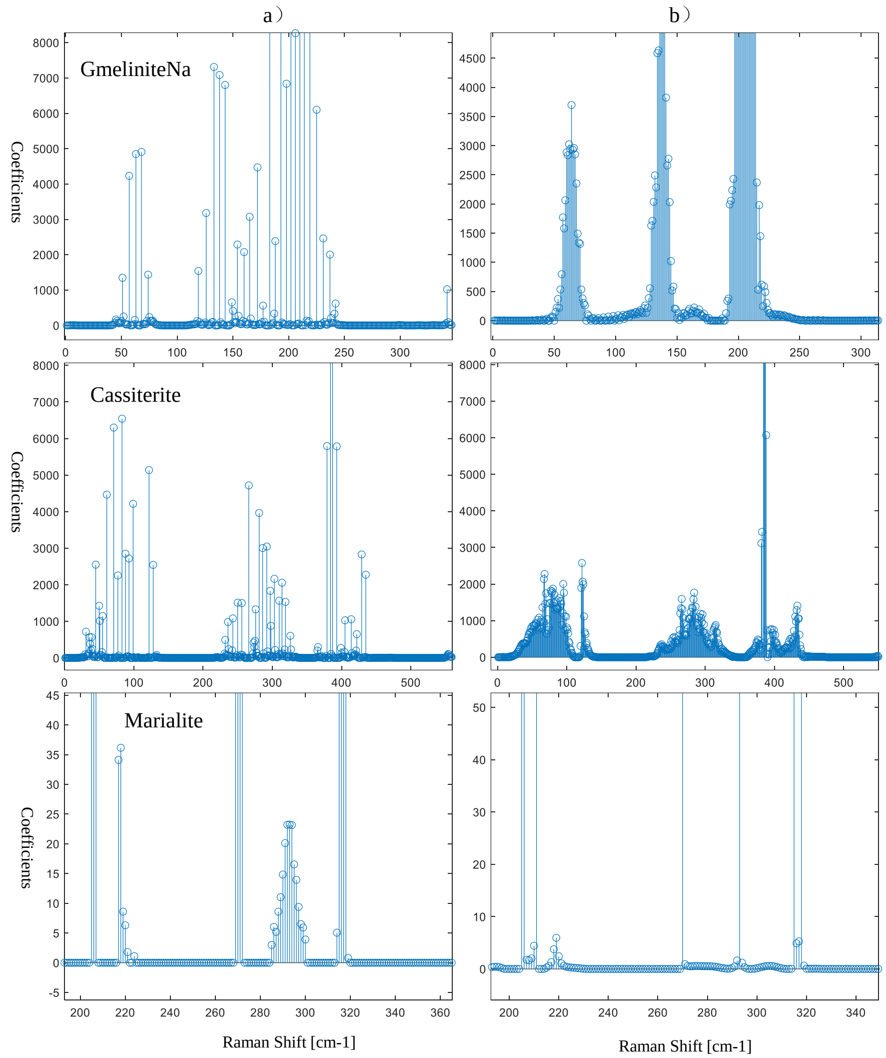

Figure S-8: The sparse coefficients for three mineral Raman datasets, a) SBL-BC, b) FBSL-BC.

Tables

Table S-1: Comparison of averaged RMSECV among airPLS ($\lambda^{\text{air}} = 10^8$), arPLS ($\lambda^{\text{ar}} = 10^5$), SSFBCSP ($\lambda_1 = 10^4$ and $\lambda_2 = 10^{-2}$), SBL-BC ($\rho = 10^5$) and FBSL-BC.

	Moisture	Oil	Protein	Starch
airPLS	0.0418	0.0421	0.0641	0.1633
arPLS	0.0485	0.0404	0.0721	0.1590
SSFBCSP	0.0462	0.0396	0.0640	0.1549
SBL-BC	0.0451	0.0386	0.0643	**0.1442**
FBSL-BC	**0.0403**	**0.0374**	**0.0611**	0.1579

Table S-2: Comparison of averaged RMSEP results among airPLS ($\lambda^{\text{air}} = 10^8$), arPLS ($\lambda^{\text{ar}} = 10^5$), SSFBCSP ($\lambda_1 = 2 \times 10^5$ and $\lambda_2 = 10^{-2}$), SBL-BC ($\rho = 10^5$) and FBSL-BC.

	Moisture	Oil	Protein	Starch
airPLS	0.0676	0.0684	0.1113	0.2741
arPLS	0.0741	0.0664	0.1214	0.2620
SSFBCSP	0.0712	0.0662	0.1091	0.2635
SBL-BC	0.0700	**0.0609**	0.1019	**0.2545**
FBSL-BC	**0.0684**	0.0627	**0.0981**	0.2729